

A MICROSTRUCTURAL APPROACH TO MODELLING INELASTIC EFFECTS IN FIBRED BIOLOGICAL TISSUES

Estefanía Peña^{*†}, Pablo Sáez^{*†}, Manuel Doblaré^{*†} and Miguel A. Martínez^{*†}

^{*}Group of Structural Mechanics and Materials Modeling.
Aragón Institute of Engineering Research (I3A). University of Zaragoza.
María de Luna, 3. E-50018 Zaragoza, Spain.
e-mail: fany@unizar.es

[†]CIBER de Bioingeniería, Biomateriales y Nanomedicina (CIBER-BBN)

Key words: Soft tissue, Microsphere, Affine deformations, damage and blood vessels

Abstract. Enormous progress has been made during recent years in the phenomenological modelling of soft tissue. In general, three important softening phenomena associated with biological tissues may be distinguished. First, there is the dependence of the mechanical response on the previously attained maximum load level. This is quite similar to the well-known Mullins effect in rubber-like materials. Another typical phenomenon known as permanent set is characterized by residual strains after unloading. Finally, there is the softening behaviour resulting from fibre rupture and matrix disruption associated with material damage. There are several phenomenological constitutive models able to describe the failure of soft tissues from a macroscopic point of view. In this contribution a three-dimensional micro-sphere-based constitutive model for anisotropic fibrous soft biological tissue is presented, including elastic anisotropy as well as inelastic effects (softening, preconditioning and damage). The link between micro-structural inelastic contribution of the collagen fibers and macroscopic response is achieved by means of computational homogenization, involving numerical integration over the surface of the unit sphere. In order to deal with the random distribution of the fibrils within the fiber, a von Mises probability function is incorporated, and the mechanical behavior of the fibrils is defined by an exponential-type model. The inelastic effects in soft biological tissues were modeled by internal variables that characterize the structural state of the material.

1 INTRODUCTION

Enormous progress has been made during recent years in the phenomenological modelling of soft tissue. In general, three important softening phenomena associated with biological tissues may be distinguished. First, there is the dependence of the mechanical response on the previously attained maximum load level. This is quite similar to the

well-known Mullins effect in rubber-like materials. Another typical phenomenon known as permanent set is characterized by residual strains after unloading. Finally, there is the softening behaviour resulting from fibre rupture and matrix disruption associated with material damage [15, 3, 30].

There are several constitutive models able to describe the failure of soft tissues [17, 20, 25, 40, 5, 34, 37, 36, 38, 21, 11]. Balzani et al. [5] assumed that discontinuous damage occurs in arterial walls and mainly along the fiber direction. Rodríguez et al. [34, 33] introduced a stochastic-structurally based damage model for fibrous soft tissues. Only a few constitutive models have been derived to describe the loading-unloading softening behavior of soft tissues [15, 10, 33, 12, 29, 21, 31]. Franceschini et al. [15] and Horgan and Saccomandi [19] proposed an isotropic pseudoelastic model for soft tissues using isotropic and anisotropic elastic strain energy functions respectively. Calvo et al. [10] proposed an uncoupled directional damage model for fibred biological soft tissues that considers different damage evolutions for the matrix and for the different fiber families. In Li and Robertson [21] two damage mechanisms are coupled in a multiplicative manner. Peña et al. [31] showed that continuum damage mechanics models can reproduce the softening behavior during unloading or reloading only for low dissipative effects. Ehret and Itskov [12] presented a model that reproduces the softening behavior including all the tissue dissipative effects (permanent set also). However, the main drawback of this model is its use of non-standard invariants that leads to a very complicated approach. The model is not able to reproduce the damage process. Peña and Doblare [29] present a very simple pseudo-elastic anisotropic model to reproduce the softening behavior exhibited in soft biological tissues without permanent set. However the pseudo-elastic model is not able to reproduce the failure region as a result of the bond rupture and complete damage while Continuum Damage Mechanics (CDM) and other models can. Finally, Peña [27] developed a phenomenological model that includes all these phenomena in a macro-estructural approach.

The high complexity of biological tissues requires mechanical models that include information of the underlying constituents and look for the physics of the whole processes within the material. This behavior of the micro-constituents can be taken into macroscopic models by means of computational homogenization. It is in this context where the microsphere-based approach acquires high relevance. [24], [23] and [16] used the microsphere approach with emphasis on elastomers. Later [2] focus on the anisotropy of the soft biological tissues.

In this contribution a three-dimensional micro-sphere-based constitutive model for anisotropic fibrous soft biological tissue is presented, including elastic anisotropy as well as inelastic effects (softening, preconditioning and damage). The link between micro-structural inelastic contribution of the collagen fibers and macroscopic response is achieved by means of computational homogenization, involving numerical integration over the surface of the unit sphere. In order to deal with the random distribution of the fibrils within the fiber, a von Mises probability function is incorporated, and the mechanical behavior of

the fibrils is defined by an exponential-type model. The inelastic effects in soft biological tissues were modelled by internal variables that characterize the structural state of the material.

2 MICROSTRUCTURAL APPROACH FOR HYPERELASTIC MEDIA

2.1 KINEMATICS

Let $\mathcal{B}_0 \subset \mathbb{E}^3$ be a reference or rather material configuration of a body B of interest. The notation $\varphi : \mathcal{B}_0 \times \mathcal{T} \rightarrow \mathcal{B}_t$ represents the one to one mapping, continuously differentiable, transforming a material point $\mathbf{X} \in \mathcal{B}_0$ to a position $\mathbf{x} = \varphi(\mathbf{X}, t) \in \mathcal{B}_t \subset \mathbb{E}^3$, where \mathcal{B}_t represents the deformed configuration at time $t \in \mathcal{T} \subset \mathbb{R}$. The mapping φ represents a motion of the body B that establishes the trajectory of a given point when moving from its reference position \mathbf{X} to \mathbf{x} . The two-point deformation gradient tensor is defined as $\mathbf{F}(\mathbf{X}, t) := \nabla_{\mathbf{X}}\varphi(\mathbf{X}, t)$, with $J(\mathbf{X}) = \det(\mathbf{F}) > 0$ the local volume variation. It is sometimes useful to consider the multiplicative decomposition of \mathbf{F}

$$\mathbf{F} := J^{1/3}\mathbf{I} \cdot \bar{\mathbf{F}}. \quad (1)$$

Hence, deformation is split into a dilatational part, $J^{1/3}\mathbf{I}$, where \mathbf{I} represents the second-order identity tensor, and an isochoric contribution, $\bar{\mathbf{F}}$, so that $\det(\bar{\mathbf{F}}) = 1$ [14]. With these quantities at hand, the isochoric counterparts of the right and left Cauchy-Green deformation tensors associated with $\bar{\mathbf{F}}$ are defined as $\bar{\mathbf{C}} := \bar{\mathbf{F}}^T \cdot \bar{\mathbf{F}} = J^{-2/3}\mathbf{C}$.

Furthermore, let \mathbf{r} be a vector in the reference configuration. The so called push-forward operator, associated to the motion, maps this vector field in $\bar{\mathbf{t}} \in \Omega$, in the deformed configuration. Assuming that \mathbf{r} is affected only by the isochoric part of \mathbf{F}

$$\bar{\mathbf{t}} = \bar{\mathbf{F}} \cdot \mathbf{r} = J^{-1/3}\mathbf{t} \quad \text{with} \quad \|\bar{\mathbf{t}}\| = \bar{\lambda} = J^{-1/3} \|\mathbf{t}\|, \quad (2)$$

where $\bar{\mathbf{t}}$ represents the isochoric push-forward of the material vector \mathbf{r} and $\bar{\lambda}$ the isochoric stretch in the direction of \mathbf{r} [18].

2.2 HYPERELASTIC FRAMEWORK

The free energy density function is given by a scalar-valued function Ψ defined per unit reference volume in the reference configuration and for isothermal processes. [14] postulated the additive decoupled representation of this SEDF in volumetric and isochoric parts as

$$\Psi = \Psi_{\text{vol}} + \Psi_{\text{ich}}. \quad (3)$$

As discussed in the introduction, soft biological tissues are a highly non-linear anisotropic materials. To differentiate between the isotropic and the anisotropic parts, the free energy density function can be split up again as

$$\Psi = \Psi_{\text{vol}} + \Psi_{\text{iso}} + \Psi_{\text{ani}}, \quad (4)$$

where Ψ_{vol} describes the free energy associated to changes of volume, Ψ_{iso} is the isotropic contribution of the free energy (usually associated to the ground matrix) and Ψ_{ani} takes into account the isochoric anisotropic contribution (associated to the fibers) [35]. This strain-energy density function must satisfy the principle material frame invariance

$$\Psi(\mathbf{C}, \mathbf{M}, \mathbf{N}) = \Psi(\mathbf{Q} \cdot \mathbf{C}, \mathbf{Q} \cdot \mathbf{M}, \mathbf{Q} \cdot \mathbf{N}) \text{ for all } [\mathbf{C}, \mathbf{Q}] \in [\mathbb{S}_+^3 \times \mathbb{Q}_+^3]. \quad (5)$$

The second Piola-Kirchhoff stress tensor is obtained by derivation of (3) with respect to the right Cauchy-Green tensor [22]. Thus, the stress tensor consists of a purely volumetric and a purely isochoric contribution, i.e. \mathbf{S}_{vol} and \mathbf{S}_{ich} , so the total stress is

$$\begin{aligned} \mathbf{S} = \mathbf{S}_{\text{vol}} + \mathbf{S}_{\text{ich}} &= 2 \frac{\partial \Psi_{\text{vol}}(J)}{\partial \mathbf{C}} + 2 \frac{\partial \Psi_{\text{ich}}(\bar{\mathbf{C}}, \mathbf{M}, \mathbf{N})}{\partial \bar{\mathbf{C}}} \\ &= 2 \left[\frac{\partial \Psi_{\text{vol}}(J)}{\partial J} \frac{\partial J}{\partial \mathbf{C}} + \frac{\partial \Psi_{\text{ich}}(\bar{\mathbf{C}}, \mathbf{M}, \mathbf{N})}{\partial \bar{\mathbf{C}}} \frac{\partial \bar{\mathbf{C}}}{\partial \mathbf{C}} \right] = J p \mathbf{C}^{-1} + 2 \sum_{j=1,2,4,6} \mathbf{P} : \frac{\partial \Psi_{\text{ich}}}{\partial \bar{I}_j} \frac{\partial \bar{I}_j}{\partial \bar{\mathbf{C}}}, \end{aligned} \quad (6)$$

where the second Piola-Kirchhoff stress \mathbf{S} consists of a purely volumetric contribution and a purely isochoric one. Moreover, one obtains the following noticeable relations $\partial_{\mathbf{C}} J = \frac{1}{2} J \mathbf{C}^{-1}$ and $\mathbf{P} = \partial_{\bar{\mathbf{C}}} \bar{\mathbf{C}} = J^{-2/3} [\mathbf{I} - \frac{1}{3} \mathbf{C} \otimes \mathbf{C}^{-1}]$. \mathbf{P} is the fourth-order projection tensor and \mathbf{I} denotes the fourth-order unit tensor, which, in index notation, has the form $I_{IJKL} = \frac{1}{2} [\delta_{IK} \delta_{JL} + \delta_{IL} \delta_{JK}]$. Application of the fourth-order projection tensor \mathbf{P} furnishes the physically correct deviatoric operator in the Lagrangian description, so that $[\mathbf{P} : (\cdot)] : \mathbf{C} = \mathbf{0}$ [13]. Note that it is possible to obtain the Cauchy stress tensor by applying the push-forward operation to (6) $\boldsymbol{\sigma} = J^{-1} \boldsymbol{\chi}_*(\mathbf{S})$ [22].

Based on the kinematic decomposition of the deformation gradient tensor, the tangent operator, also known as the elasticity tensor when dealing with elastic constitutive laws, is defined in the reference configuration as

$$\mathbf{C} = 2 \frac{\partial \mathbf{S}(\mathbf{C}, \mathbf{M}, \mathbf{N})}{\partial \mathbf{C}} = \mathbf{C}_{\text{vol}} + \mathbf{C}_{\text{ich}} = 4 \left[\frac{\partial^2 \Psi_{\text{vol}}(J)}{\partial \mathbf{C} \otimes \partial \mathbf{C}} + \frac{\partial^2 \Psi_{\text{ich}}(\bar{\mathbf{C}}, \mathbf{M}, \mathbf{N})}{\partial \bar{\mathbf{C}} \otimes \partial \bar{\mathbf{C}}} \right]. \quad (7)$$

Note that its spatial counterpart of (7) is obtained from the application of the push-forward operation to (7) $\mathbf{c} = J^{-1} \boldsymbol{\chi}_*(\mathbf{C})$ [8].

2.3 MICROSHERE BASED MODEL

During the last years the most widely used approach for modeling anisotropy in soft tissues has been representing fiber directions by means of an invariant formulation. Lately, the use of statistical distributions has increased, being this latter also adopted in the present work. Furthermore, a microsphere-based approach has been used at a micro scale level. The microsphere approach tries to capture micro-structural information and transfer it into the macroscopic behavior via a homogenization scheme over the unit sphere \mathbb{U}^2 . In this approach, \mathbb{U}^2 is discretized into m directions $\{\mathbf{r}^i\}_{i=1\dots m}$ that are weighted by factors

$\{w^i\}_{i=1\dots m}$, where $\langle \mathbf{r} \rangle \approx \sum_{i=1}^m w^i \mathbf{r}^i = \mathbf{0}$ and $\langle \mathbf{r} \otimes \mathbf{r} \rangle \approx \sum_{i=1}^m w^i \mathbf{r}^i \otimes \mathbf{r}^i = \frac{1}{3} \mathbf{I}$. So an integral over the unit sphere \mathbb{U}^2 can be approximated by

$$\langle (\bullet) \rangle = \frac{1}{4\pi} \int_{\mathbb{U}^2} (\bullet) dA \approx \sum_{i=1}^m w^i (\bullet)^i. \quad (8)$$

The term 4π is a normalization factor, result of the surface integral $\int_0^\theta \int_0^\phi \sin(\theta) d\theta d\phi$ over the unit sphere. The unit vectors can be expressed in terms of the spherical coordinates $\theta \in [0, \pi]$ and $\phi \in [0, 2\pi]$ as $\mathbf{r} = \sin(\theta)\cos(\phi)\mathbf{e}_x + \sin(\theta)\sin(\phi)\mathbf{e}_y + \cos(\theta)\mathbf{e}_z$ with $\{\mathbf{e}_x, \mathbf{e}_y, \mathbf{e}_z\}$ the reference Cartesian system. Previous works [6, 1, 2] have used and compared different number of integration directions for isotropic and anisotropic functions and, in view of the results therein, 368 directions will be used in all the problems simulated in this work that demonstrated to provide sufficiently accurate results for relatively highly anisotropic materials (see [1]).

As detailed above, the anisotropic part of the SEDF is related to the fibers in the material. In a general situation with N families of fibers the anisotropic part of the SEDF can be expressed as

$$\Psi_{\text{ani}} = \sum_{j=1}^N \Psi_{\text{f}}^j = \sum_{j=1}^N \left[\frac{1}{4\pi} \int_{\mathbb{U}^2} n \rho_{\text{f}} \psi_{\text{f}} dA \right]_j, \quad (9)$$

where Ψ_{f}^j is the strain energy density function for the j -nth fiber family, n the chain density, ρ_{f} a statistical value associated with the fibrils dispersion and ψ_{f} the free energy density function of the fibril. We will adopt an affine assumption for the integration directions (compare [24]), in spite of the model used for the micro fibers, as for example a non-affine eight-chain model [4]. Since an analytical integration of (9) is not possible in general, a discretization of this equation is used

$$\Psi_{\text{ani}} \approx \sum_{j=1}^N \left[\sum_{i=1}^m n \rho_i w^i \psi(\bar{\lambda}_i) \right], \quad (10)$$

where $\bar{\lambda}_i$ and $\psi(\bar{\lambda}_i)$ are the stretch ratio and the free energy density function associated to each integration direction.

In order to obtain the macroscopic contribution to the Kirchhoff stresses and the elasticity tensor for a family of fibers, the SEDF has been written in terms of stretches, rather than the classical invariant's function [26]. The equations for the Kirchhoff stress and the elasticity tensors in the spatial configuration are expressed as:

$$\boldsymbol{\tau}_f = \sum_{i=1}^m [n \rho_i \psi'_i \bar{\lambda}_i^{-1} \bar{\mathbf{t}} \otimes \bar{\mathbf{t}}] w^i \quad (11)$$

and

$$\mathbf{c}_f = \sum_{i=1}^m [n \rho_i [\psi''_i - \psi'_i \bar{\lambda}_i^{-1}] \bar{\lambda}_i^{-2} \bar{\mathbf{t}} \otimes \bar{\mathbf{t}} \otimes \bar{\mathbf{t}} \otimes \bar{\mathbf{t}}] w^i \quad (12)$$

where ψ'_i and ψ''_i are the first and second derivative of the fibril energy function with respect to λ_i . Additional details are given in Appendix A.

2.4 MATERIAL BEHAVIOR

The definition of a given material in the hyperelastic framework is associated therefore to establishing a free energy density function for each part of the above discussed splitting. Here, we have used

$$\Psi = \Psi_{\text{vol}}(J) + \Psi_{\text{iso}}(\bar{I}_1) + \Psi_{\text{ani}}(n, \rho, \bar{\lambda}), \quad (13)$$

$$\Psi_{\text{vol}}(J) = \frac{1}{D} \ln^2(J), \quad (14)$$

$$\Psi_{\text{iso}}(\bar{I}_1) = \mu[\bar{I}_1 - 3] \text{ and} \quad (15)$$

$$\Psi_{\text{ani}}(n, \rho, \bar{\lambda}) = \langle n \rho_f \psi_f \rangle. \quad (16)$$

The matrix is known to be composed of an important water content, which results in an almost incompressible behavior, so the volumetric part of the energy density function enforces the quasi-incompressibility constraint depending on the value of the penalty parameter D (14). The matrix contributes to the overall behavior through the volumetric and the isotropic parts of the energy density function (15).

The contribution of each single collagen fibril in the micro scale is here assumed as a first approach, to be defined by an exponential-type function, widely used in macroscopic approaches [18]. In [1] a comparison between this phenomenological function and the worm-like chain model in the microsphere framework is discussed. Note that, although the integration directions are mathematically identified with the homogenization directions, they can be physically associated to the contribution of a fibril. The free density energy associated to each fibril or, equivalently, to each integration direction, is assumed as

$$n\psi_i^j(\bar{\lambda}_i) = \begin{cases} 0, & \text{if } \bar{\lambda}_i < 1 \\ \frac{k_1}{2k_2} [\exp(k_2[\bar{\lambda}_i^2 - 1]^2)] & \text{if } \bar{\lambda}_i \geq 1 \end{cases} \quad (17)$$

2.5 THE VON MISES ORIENTATION DISTRIBUTION FUNCTION

Regarding the anisotropic part of the model (16), a statistical distributions of the fibrils around a preferential orientation is considered through a von Mises statistical function. This orientation distribution function is denoted by ρ and has some interesting properties such as symmetry $\rho(\mathbf{r}; \mathbf{a}) = \rho(-\mathbf{r}; \mathbf{a})$ and rotational symmetry with respect to the preferred orientation \mathbf{a} , which can be expressed as $\rho(\mathbf{Q} \cdot \mathbf{r}; \mathbf{a}) = \rho(\mathbf{r}; \mathbf{a}) \forall \mathbf{Q} \in \mathbb{Q}_+^3$. Note that \mathbf{a} could be oriented in any direction of the space leading to a mismatch angle $w = \arccos(\mathbf{r} \cdot \mathbf{a})$. A π -periodic von Mises orientation density function (ODF) (18) has been adopted in this work to take into account the fibrils dispersion [1]

$$\rho(\theta) = 4\sqrt{\frac{b}{2\pi}} \frac{\exp(b[\cos(2\theta) + 1])}{\text{erfi}(\sqrt{2b})}, \quad (18)$$

where the concentration parameter $b \in \mathbb{R}^+$ is a measure of the anisotropy. $b \rightarrow 0$ represents an isotropic material, and $b \rightarrow \infty$ a transversally isotropic one. $\text{erfi}(x)$ is the imaginary error function approximated by a sufficiently large number of terms within its MacLaurin series expansion, which can be written as

$$\text{erfi}(x) \approx \pi^{-1/2} \left[2x + \frac{2x^3}{3} + \sum_{j=3}^k \frac{x^{2j-1}}{a(j)} \right], \quad (19)$$

with $a(j) = 0.5[2j - 1][j - 1]!$ [39] provides a 60 term expansion, sufficiently accurate for values of $b \leq 20$. Figure 1 shows the spherical representation of two distributions for different values of b .

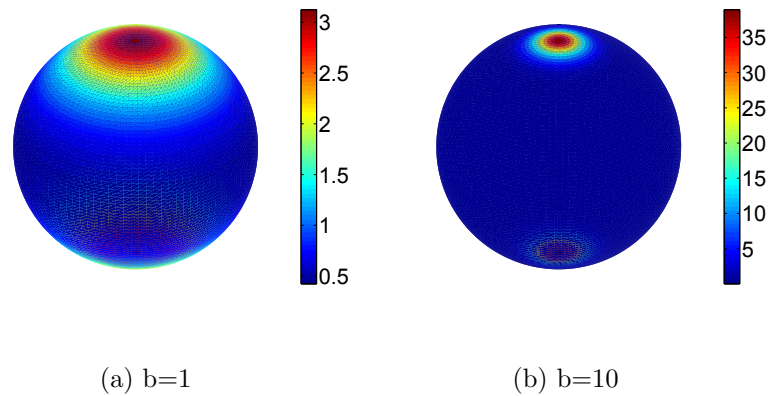


Figure 1: Shape of the von Mises ODF for $b=1$ and $b=10$.

3 INELASTIC CONSTITUTIVE MODEL

The experimental results suggest that just like the elastic properties, the inelastic behavior of soft tissues is also characterized by anisotropy [3, 31, 28, 30]. Accordingly, a suitable constitutive model should account for this directional dependence and take into account the different alteration mechanisms associated with this anisotropy. The phenomenological inelastic model should include the Mullins effect, the permanent set resulting from the residual strains after unloading, and the fibre and matrix disruption associated to supraphysiological loads or strains [9].

3.1 Hypothesis of the model

To model these inelastic processes, we apply the following considerations:

- We have modified the equation (17) by the parameter w_i

$$n\psi_i^j(\bar{\lambda}_i) = \begin{cases} 0, & \text{if } \bar{\lambda}_i < 1 \\ \frac{k_1}{2k_2} [\exp(k_2[\bar{\lambda}_i^2 - w_i]^2)] & \text{if } \bar{\lambda}_i \geq 1 \end{cases} \quad (20)$$

that governs the anisotropic contribution to the global mechanical response of the tissue only when stretched, that is, $\bar{\lambda}_i^2 > w_i$ [27].

- Finally, we modified this parameter that changes independently from each direction to take into account structural alterations along the fiber direction. With this modification, we can reproduce at the same time the softening behavior and the permanent set presented in this kind of tissue.

The second law of thermodynamics asserts a non-negative rate of entropy production. Using standard arguments based on the Clausius-Duhem inequality [22]

$$\mathcal{D}_{int} = -\dot{\Psi} + \frac{1}{2} \mathbf{S} : \dot{\mathbf{C}} \geq 0 \quad (21)$$

yields

$$\mathcal{D}_{int} = - \sum_{j=1}^N \left[\sum_{i=1}^m \frac{\partial \psi_{j,0}^i(\bar{\lambda}^i)}{\partial w_i} \dot{w}_i \right] \geq 0 \quad (22)$$

where the thermodynamic forces are

$$f_{w_i} = - \frac{\partial \psi_{j,0}^i(\bar{\lambda}^i)}{\partial w_i} \quad (23)$$

The thermodynamic force f_{w_i} is conjugated to the internal variable w_i , so the process could be controlled by f_{w_i} instead of w_i (see e.g. [10]).

3.2 Evolution of the internal variables

For the softening variables w_i , we consider the following criteria

$$\Upsilon_i(\mathbf{C}(t), \Gamma_{i_t}) = \frac{\partial \psi_{j,0}^i(\bar{\lambda}^i)}{\partial \bar{\lambda}^i} - \Gamma_{i_t} = \Gamma_i - \Gamma_{i_t} \leq 0 \quad (24)$$

where $\Gamma_i = \frac{\partial \psi_{j,0}^i(\bar{\lambda}^i)}{\partial \bar{\lambda}^i}$ is the softening stress release rate at time $t \in \mathbb{R}_+$ and Γ_{i_t} signifies the softening threshold (stress barrier) at current time t for matrix and fibers

$$\Gamma_{i_t} = \max_{sr \in (-\infty, t)} \frac{\partial \psi_{j,0}^i(\bar{\lambda}^i)}{\partial \bar{\lambda}^i} \quad (25)$$

The equation $\Upsilon_i(\mathbf{C}(t), \Gamma_{i_t}) = 0$ defines a softening surface in the strain space. With these means at hand, we finally propose the following set of rate equations for an evolution of the softening variables

$$\dot{w}_i \doteq \begin{cases} \kappa_i \dot{\Gamma}_{i_t} & \text{if } \Upsilon = 0 \quad \text{and} \quad \mathbf{N}_i : \dot{\mathbf{C}} > 0 \\ 0 & \text{otherwise} \end{cases} \quad (26)$$

Let us now consider softening functions of the simple form

$$w_i = \kappa_i \Gamma_{i_t} + 1 \quad (27)$$

where κ_i is the only parameter to define the softening mechanism in each fiber direction.

4 NUMERICAL EXAMPLE

The principal aim of this section is to illustrate the performance and the physical mechanics involved in the above presented model. With this purpose, a uniaxial test of an incompressible biological tissue is computed in this example. Only one family of fibres is defined along the X direction. The softening evolution is formulated in (27). The tissue was subjected to stepwise uniaxial loading in fiber direction with five stretch controlled cycles where the stretch was 1.4, 1.6, 1.8, 2.0, 2.2.

| μ | k_1 | k_2 | w_i^0 | κ_i |
|-------|--------|--------|---------|------------|
| 0.28 | 1.1226 | 1.5973 | 1.1 | 0.003 |

Table 1: Material, damage and softening parameters for uniaxial simple tension. μ and k_1 are in MPa, and other parameters are dimensionless

Figure 2 shows the results. It is possible to observe the softening phenomena during unloading that increases when the maximum load increases showing the typical Mullins' effect observed in soft biological tissues. Finally, the permanent set is presented in the model when the stress are null, and, again the residual stretch increases when the maximum load increases.

5 CONCLUSIONS

The aim of this work is to present the complete formulation of a softening model within an anisotropic microsphere-based approach in order to a better characterization of this phenomenon in biological soft tissues. We consider the weight factors w_i (as internal variables characterizing the structural state of the material with different evolution rule in each integration direction of the microsphere. The limitations of the study include: (1) the need for a suitable experimental plan to obtain the many parameters involved; (2) the softening behavior of biological tissues is also related to viscoelastic effects; (3) one numerical problem concerning the finite element implementation should be addressed.

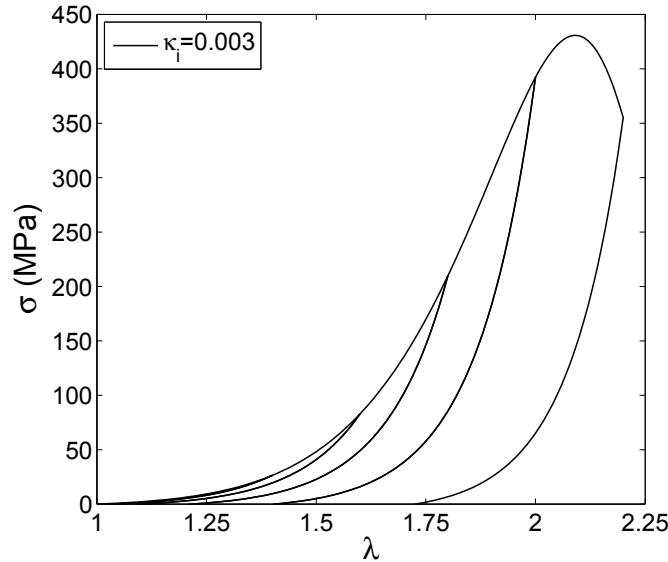


Figure 2: Uniaxial stress response under cyclic uniaxial tension in X direction.

This is related with the necessity of regularizing the ill-posed numerical problem [7] where the loss of ellipticity/hyperbolicity of the governing equations with softening can lead to pathological mesh-sensitivity [32]. In spite of these limitations, the one dimensional character of the constitutive equations applied at the micro-level offers huge possibilities, due to its simplicity and the possibility of incorporating other micro-structural variables.

6 ACKNOWLEDGEMENTS

Support of the Spanish Ministry of Research and Innovation through the research project DPI2010-20746-C03-01 and through the grant BES-2009-028593 to P. Sáez, as well as the support of the Instituto de Salud Carlos III through the CIBER are highly appreciated. CIBER-BBN is an initiative funded by the VI National R&D&I Plan 2008-2011, Iniciativa Ingenio 2010, Consolider Program, CIBER Actions and financed by the Instituto de Salud Carlos III with assistance from the European Regional Development Fund.

References

- [1] Alastrué, V., Martínez, M. A., Menzel, A., and Doblaré, M. (2009a). On the use of non-linear transformations for the evaluation of anisotropic rotationally symmetric directional integrals. application to the stress analysis in fibred soft tissues. *Int J Numer Meth Biom Eng*, 79:474–504.
- [2] Alastrué, V., Martínez, M. A., Doblaré, M., and Menzel, A. (2009b). Anisotropic

- micro-sphere-based finite elasticity applied to blood vessel modelling. *J Mech Phys Solids*, 57:178–203.
- [3] Alastrué, V., Peña, E., Martínez, M. A., and Doblaré, M. (2008). Experimental study and constitutive modelling of the passive mechanical properties of the ovine infrarenal vena cava tissue. *J Biomech*, 41:3038–3045.
- [4] Arruda, E. M. and Boyce, M. C. (1993). A three-dimensional constitutive model for the large stretch behavior of rubber elastic materials. *J Mech Phys Solids*, 41(2):389–412.
- [5] Balzani, D., Schröder, J., and Gross, D. (2006). Simulation of discontinuous damage incorporating residual stress in circumferentially overstretched atherosclerotic arteries. *Acta Biomater*, 2:609–618.
- [6] Bažant, P. and Oh, B. H. (1986). Efficient numerical integration on the surface of a sphere. *ZAMM-Z Angew Math Mech*, 66:37–49.
- [7] Bazant, Z. P. and Jirasek, M. (2002). Nonlocal integral formulations of plasticity and damage: Survey of progress. *J Eng Mech*, 128:1119–1149.
- [8] Bonet, J. and Wood, R. D. (2008). *Nonlinear Continuum Mechanics for Finite Element Analysis*. Cambridge University Press, Cambridge.
- [9] Calvo, B., Peña, E., Martins, P., Mascarenhas, T., Doblare, M., Natal, R., and Ferreira, A. (2009). On modelling damage process in vaginal tissue. *J Biomech*, 42:642–651.
- [10] Calvo, B., Peña, E., Martínez, M. A., and Doblaré, M. (2007). An uncoupled directional damage model for fibered biological soft tissues. Formulation and computational aspects. *Int J Numer Meth Engng*, 69:2036–2057.
- [11] Ciarletta, P. and Ben-Amar, M. (2009). A finite dissipative theory of temporary interfibrillar bridges in the extracellular matrix of ligaments and tendons. *J R Soc Interface*, 6:909–92.
- [12] Ehret, A. E. and Itskov, M. (2009). Modeling of anisotropic softening phenomena: Application to soft biological tissues. *Int J Plasticity*, 25:901–919.
- [13] Federico, S. (2010). Volumetric-distortional decomposition of deformation and elasticity tensor. *Math Mech Solids*, 15:672–690.
- [14] Flory, P. J. (1961). Thermodynamic relations for high elastic materials. *Trans Faraday Soc*, 57:829–838.

- [15] Franceschini, G., Bigoni, D., Regitnig, P., and Holzapfel, G. A. (2006). Brain tissue deforms similarly to filled elastomers and follows consolidation theory. *J Mech Phys Solids*, 54:2592–2620.
- [16] Göktepe, S. and Miehe, C. (2005). A micro-macro approach to rubber-like materials—part iii: the micro-sphere model of finite rubber viscoelasticity. *J Mech Phys Solids*, 53:2259–2283.
- [17] Hokanson, J. and Yazdani, S. (1997). A constitutive model of the artery with damage. *Mech Res Commun*, 24:151–159.
- [18] Holzapfel, G. A. (2000). *Nonlinear Solid Mechanics*. Wiley, New York.
- [19] Horgan, C. O. and Saccomandi, G. (2005). A new constitutive theory for fiber-reinforced incompressible nonlinearly elastic solids. *J Mech Phys Solids*, 53:1985–2025.
- [20] Hurschler, C., Loitz-Ramage, B., and Vanderby, R. (1997). A structurally based stress-stretch relationship for tendon and ligament. *ASME J Biomech Eng*, 119:392–399.
- [21] Li, D. and Robertson, A. M. (2009). A structural multi-mechanism damage model for cerebral arterial tissue. *ASME J Biomech Eng*, 131:101013 1–8.
- [22] Marsden, J. E. and Hughes, T. J. R. (1994). *Mathematical Foundations of Elasticity*. Dover, New York.
- [23] Miehe, C. and Göktepe, S. (2005). A micro-macro approach to rubber-like materials—part ii: the micro-sphere model of finite rubber viscoelasticity. *J Mech Phys Solids*, 53:2231–2258.
- [24] Miehe, C., Göktepe, S., and Lulei, F. (2004). A micro-macro approach to rubber-like materials—part i: the non-affine micro-sphere model of rubber elasticity. *J Mech Phys Solids*, 52:2617–2660.
- [25] Natali, A. N., Pavan, P. G., Carniel, E. L., Luisiano, M. E., and Tagliavero, G. (2005). Anisotropic elasto-damage constitutive model for the biomechanical analysis of tendons. *Med Eng Phys*, 27:209–214.
- [26] Ogden, R. W. (1996). *Non-linear Elastic Deformations*. Dover, New York.
- [27] Peña, E. (2011). Prediction of the softening and damage effects with permanent set in fibrous biological materials. *J Mech Phys Solids*, page Accepted.
- [28] Peña, E., Alastrue, V., Laborda, A., Martínez, M. A., and Doblaré, M. (2010). A constitutive formulation of vascular tissue mechanics including viscoelasticity and softening behaviour. *J Biomech*, 43:984–989.

- [29] Peña, E. and Doblare, M. (2009). An anisotropic pseudo-elastic approach for modelling Mullins effect in fibrous biological materials. *Mech Res Commun*, 36:784–790.
- [30] Peña, E., Martins, P., Mascarenhas, T., Natal-Jorge, R. M., Ferreira, A., Doblaré, M., and Calvo, B. (2011a). Mechanical characterization of the softening behavior of human vaginal tissue. *J Mech Behav Biomed*, 4:275–283.
- [31] Peña, E., Peña, J. A., and Doblaré, M. (2009). On the Mullins effect and hysteresis of fibered biological materials: A comparison between continuous and discontinuous damage models. *Int J Solids Struct*, 46:1727–1735.
- [32] Peña, J. A., Martínez, M. A., and Peña, E. (2011b). A formulation to model the nonlinear viscoelastic properties of the vascular tissue. *Acta Mech*, 217:63–74.
- [33] Rodríguez, J. F., Alastrue, V., and Doblaré, M. (2008). Finite element implementation of a stochastic three dimensional finite-strain damage model for fibrous soft tissue. *Comput Methods Appl Mech Engrg*, 197:946–958.
- [34] Rodríguez, J. F., Cacho, F., Bea, J. A., and Doblaré, M. (2006). A stochastic-structurally based three dimensional finite-strain damage model for fibrous soft tissue. *J Mech Phys Solids*, 54:864–886.
- [35] Spencer, A. J. M. (1971). Theory of Invariants. In *Continuum Physics*, pages 239–253. Academic Press, New York.
- [36] Vita, R. D. and Slaughter, W. S. (2007). A constitutive law for the failure behavior of medial collateral ligaments. *Biomech Model Mechanbiol*, 6:189–197.
- [37] Volokh, K. Y. (2007). Hyperelasticity with softening for modeling materials failure. *J Mech Phys Solids*, 55:2237–2264.
- [38] Volokh, K. Y. and Vorp, D. A. (2008). A model of growth and rupture of abdominal aortic aneurysm. *J Biomech*, 41:1015–1021.
- [39] Weisstein, E. W. (2004). “Erfi.” From MathWorld—A Wolfram Web Resource. <http://mathworld.wolfram.com/Erfi.html>.
- [40] Wulandana, R. and Robertson, A. M. (2005). An inelastic multi-mechanism constitutive equation for cerebral arterial tissue. *Biomech Model Mechanbiol*, 4:235–248.